

THE OFFICIAL MAGAZINE OF THE OCEANOGRAPHY SOCIETY

Oceanography

CITATION

Gregg, P.M., L.B. Hebert, L.G.J. Montési, and R.F. Katz. 2012. Geodynamic models of melt generation and extraction at mid-ocean ridges. *Oceanography* 25(1):78–88, <http://dx.doi.org/10.5670/oceanog.2012.05>.

DOI

<http://dx.doi.org/10.5670/oceanog.2012.05>

COPYRIGHT

This article has been published in *Oceanography*, Volume 25, Number 1, a quarterly journal of The Oceanography Society. Copyright 2012 by The Oceanography Society. All rights reserved.

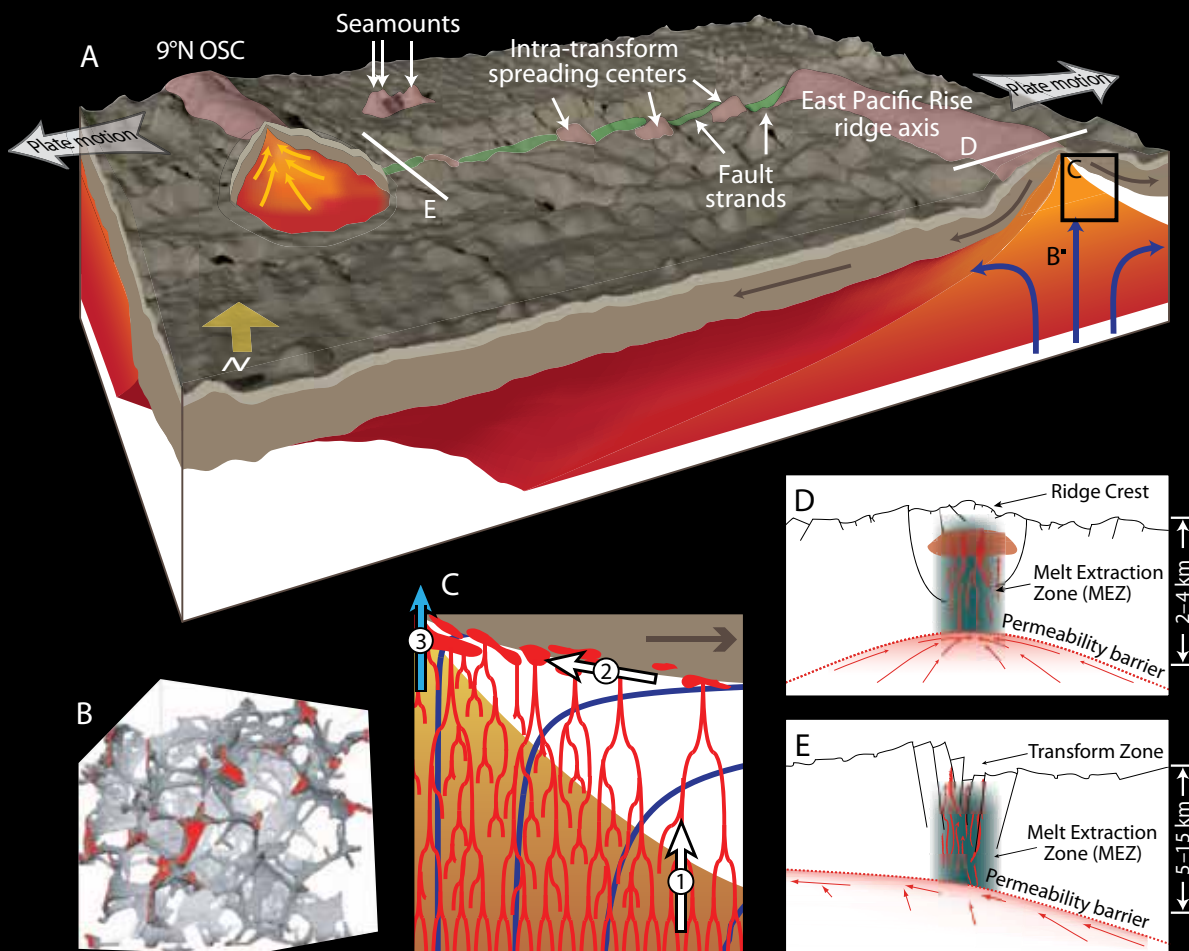
USAGE

Permission is granted to copy this article for use in teaching and research. Republication, systematic reproduction, or collective redistribution of any portion of this article by photocopy machine, reposting, or other means is permitted only with the approval of The Oceanography Society. Send all correspondence to: info@tos.org or The Oceanography Society, PO Box 1931, Rockville, MD 20849-1931, USA.



Geodynamic Models of Melt Generation and Extraction at Mid-Ocean Ridges

BY PATRICIA M. GREGG, LAURA B. HEBERT,
LAURENT G.J. MONTÉSI, AND RICHARD F. KATZ



ABSTRACT. It is widely accepted that plate divergence at mid-ocean ridges drives mantle flow, mantle melting, and the formation of new oceanic crust. However, many of the details of this process remain obscure because of the inaccessibility of the mantle to direct observation. Thus, geodynamic models are needed to provide insight into the processes that control the formation of new crust and hydrothermal circulation at mid-ocean ridges. These models allow us to test governing parameters and investigate physical hypotheses and conceptual models derived from geological, geophysical, and geochemical observations. During the span of the Ridge 2000 Program, a new generation of models was developed to calculate the width of the melt region and the extent of melting beneath mid-ocean ridges, track the pathways along which melts may migrate, and predict melt and residual mantle compositions as the system evolves. Findings from these studies illustrate the importance of melt focusing for the efficient delivery of melt to the ridge axis, the complexities of migrating melt in the vicinity of ridge offsets, and the effect of mantle rheology in model calculations.

MANTLE MELTING AT MID-OCEAN RIDGES

Most of Earth's mantle is solid due to high ambient pressures. However, melting of the mantle can occur beneath mid-ocean ridges as the solid mantle rises and decompresses in response to plate divergence. The depth of the onset of melting, melt-region width, and the maximum extent of melting are all functions of mantle temperature, its water content, and the rate at which the plates above are diverging (Asimow and Langmuir, 2003; Langmuir and Forsyth, 2007). In the fastest spreading environments, such as the southern East Pacific Rise, the melt region beneath the ridge axis is potentially hundreds

of kilometers wide and approximately 100 km deep (MELT Seismic Team, 1998). At very slow spreading ridges, the melt region may be 20 times narrower (Montési and Behn, 2007) with lower extent of melting. In either case, at the surface, new oceanic crust is generated over a narrow zone no more than a few kilometers wide (Macdonald et al., 1982; Standish and Sims, 2010).

The melting region likely controls crustal thickness variations, spreading center morphology, and major and trace element abundances in seafloor basalts. For example, cold, slow-spreading ridge environments have relatively thin crust, an axial valley, and major element compositions indicating deeper and

lower extents of melting than hot, fast-spreading environments (Langmuir and Forsyth, 2007).

Melt generation and extraction is inherently a three-dimensional process that involves the migration of melt through large regions of the mantle, across ridge offsets, to the ridge axis (Figure 1). At depth in the mantle, melt accumulates around grain boundaries, forming interconnected pathways that allow the buoyant melt to rise through the permeable mantle (Figure 1B; Zhu et al., 2011). As the extent of melting increases, melt may channelize and migrate very efficiently through the mantle at velocities of $\sim 100 \text{ m yr}^{-1}$ (Figure 1C; Kelemen et al., 1995; Hewitt and Fowler, 2009). Melt must also collect from a melt production region tens to hundreds of kilometers wide to an accretion region only 1–2 km wide along the ridge axis where it forms new crust. To explain this focusing, it is possible that permeability boundaries at the base of the lithosphere guide the melt laterally toward the ridge axis (Sparks and Parmentier, 1991).

Given the many complexities of melting the mantle and focusing the generated melt to the ridge axis, it is remarkable that observations of crustal thickness along the global ridge system are a relatively uniform 5 to 7 km away from the influence of hotspots (White et al., 2001). Only ultraslow spreading centers (Snow and Edmonds, 2007) seem to have anomalously thin crust of less than 4 km (Jokat et al., 2003). In the extreme, essentially no crust is present at the seafloor at the slowest ridges (Dick et al., 2003).

Variations in crustal thickness related to spreading-center segmentation are most pronounced at slow-spreading

Figure 1 (opposite page). Three-dimensional illustration of the melt region beneath the Siqueiros Transform Fault located at 8.5°N on the East Pacific Rise (mantle not to scale). The mantle region that is melting extends up to 100 km on either side of the East Pacific Rise axis, creating a large region from which melt is focused to the ridge. Gray arrows indicate plate motion, blue arrows mantle upwelling, and yellow arrows melt focusing. (B) At depth beneath the ridge, melt collects along grain boundaries (three-dimensional distribution of melt in an aggregate of olivine and 5% basalt imaged using high-resolution synchrotron microtomography; from Zhu et al., 2011). (C) Summary of the three steps of melt extraction: (1) rapid, subvertical migration from the melting region, possibly in channels (red lines), (2) accumulation and focusing along a permeability barrier along the base of the lithospheric plate, and (3) extraction to the surface in a melt extraction zone (MEZ, blue arrow) associated with faulting and the magma plumbing system of the ridge axis and the transform domain. (D) and (E) represent schematically the structures potentially present underneath the ridge (D) and the transform (E) with black lines representing faults (Hebert and Montési, 2011). *Siqueiros illustration by Jack Cook, © Woods Hole Oceanographic Institution*

ridges; there, the crust is thickest at segment centers (Kuo and Forsyth, 1988; Lin and Phipps Morgan, 1992). Along-axis geochemical variations are also observed, with deeper and lower extents of melting inferred from lavas extruded near ridge segment offsets (Bender et al., 1978; Reynolds and Langmuir, 1997). The geophysical and geochemical variations observed at slow-spreading ridges suggest mantle melt focusing toward segment centers and crustal redistribution of melt through diking along segments (Fialko and Rubin, 1998). By contrast, fast-spreading ridges exhibit relatively uniform crustal thickness and, in some cases, thicker crust near segment offsets such as transform faults (Van Avendonk et al., 2001; Canales et al., 2003; Gregg et al., 2007). Geochemical variations at fast-spreading ridges are subtle, with a reduced effect of ridge offsets on lava composition compared to slow-spreading ridges (Langmuir et al., 1986).

Geophysical and geochemical observations from mid-ocean ridges, field investigations of ophiolites, and experimental studies have inspired the development of integrative conceptual models of how melt initiates and moves through the mantle (Figure 1). Numerical geodynamic models have been developed to test these hypotheses. These models typically employ plate-driven passive or buoyant mantle upwelling centered beneath the ridge axis with constant or variable rheology

(Phipps Morgan, 1987; Spiegelman and McKenzie, 1987; Phipps Morgan and Forsyth, 1988; Shen and Forsyth, 1992; Forsyth, 1993). Typically, melting is assumed to start at a depth where the mantle reaches a pressure-dependent solidus temperature, and the extent of melting is assumed to increase linearly with temperature above the solidus (Reid and Jackson, 1981), although more advanced melting relationships have been devised and implemented (Ghiorso and Sack, 1995; Katz et al., 2003; Katz, 2008; Gregg et al., 2009). Models of melt migration propose that melt percolating upward through the hot, permeable mantle will pool along a low-permeability boundary (e.g., the top of the melting region, the base of the lithosphere, or the locus of plagioclase crystallization) and then migrate laterally, “uphill,” along this boundary to the ridge axis (Sparks and Parmentier, 1991; Sparks et al., 1993; Aharonov et al., 1995; Magde and Sparks, 1997; Kelemen and Aharonov, 1998).

Key modeling advances produced over the duration of the Ridge 2000 Program have targeted the problem of melt generation and extraction at mid-ocean ridges. These new geodynamic models include time-dependent processes such as ridge migration (Katz et al., 2004; Weatherley and Katz, 2010), couple petrologic modeling with geodynamic models to track melt composition (Gregg et al., 2009), and calculate detailed melt migration pathways

through the mantle (Katz, 2008; Montési et al., 2011). These models strive to test our understanding of how melt is generated, where that melt migrates, and how the mechanics of melt focusing affect the formation of new oceanic crust.

This paper puts the numerical modeling advancements during Ridge 2000 into the broader context of ridge research. It describes recent progress made in addressing three fundamental issues: (1) how melt is focused toward the spreading center, (2) how ridge segmentation affects melt generation and transport, and (3) how ridge migration affects melt focusing. These issues provide the context for our discussion of model results, data-model comparisons, and remaining uncertainties.

HOW IS MELT FOCUSED TOWARD THE SPREADING CENTER?

Consideration of melt focusing in the mantle is essential for determining the process of melt extraction and the composition of the lava erupted on the seafloor. Several mechanisms have been proposed to explain lateral transport of magma to the ridge axis over distances up to a hundred kilometers. Two well-studied mechanisms, large pressure gradients that serve to focus the flow of melt (Phipps Morgan, 1987; Spiegelman and McKenzie, 1987; Ribe, 1988) and buoyancy-driven convection (Rabinowicz et al., 1984; Buck and Su, 1989; Scott and Stevenson, 1989), rely on higher viscosities or higher porosities, respectively, than currently estimated beneath spreading centers. Finally, the mechanism most commonly invoked in recent models uses the development of a high-porosity channel along the base of

Patricia M. Gregg (greggp@geo.oregonstate.edu) is COAS Institutional Postdoc, College of Earth, Oceanic, and Atmospheric Sciences, Oregon State University, Corvallis, OR, USA. **Laura B. Hebert** is Assistant Research Scientist, Department of Geology, University of Maryland, College Park, MD, USA. **Laurent G.J. Montési** is Assistant Professor, Department of Geology, University of Maryland, College Park, MD, USA. **Richard F. Katz** is University Lecturer, Department of Earth Sciences, University of Oxford, Oxford, UK.

the sloping thermal lithosphere (Sparks and Parmentier, 1991; Spiegelman 1993a,b; Ghods and Arkani-Hamed, 2000; Katz, 2008). Other mechanisms, such as hydrofracturing (Sleep, 1988; Nicolas, 1990) and the development of a stress-induced anisotropic permeability (Phipps Morgan, 1987; Katz et al., 2006), should be studied in greater detail.

Two recent approaches have been developed to approximate melt focusing numerically. The first parameterizes the putative high-porosity channel at the base of the lithosphere and explores its effect on three-dimensional melt migration and focusing (Figure 1C; Magde and Sparks, 1997; Hebert and Montési, 2011; Montési et al., 2011). The second explicitly models both the mantle and magmatic phases, tracks melting and crystallization throughout the mantle, and predicts the focusing efficiency of channelized buoyant magma for given physical properties of the mantle, such as resistance to compaction (Katz, 2008). Up to now, such models have been restricted to two-dimensional geometry.

In permeability barrier models (Sparks and Parmentier, 1991; Hebert and Montési, 2010), a channel is assumed to form where vertically traveling melts crystallize within the thermal boundary layer (TBL), inducing decompression of the porous matrix beneath a melt-impermeable freezing boundary, or permeability barrier. The permeability barrier slopes upward toward the ridge axis, allowing melts to buoyantly migrate within the high-porosity channel and focus from a wide area into the narrow neovolcanic zone at the ridge where new crust is accreted. Channel development depends on the ratio of the length scale of the crystallization interval to the local compaction length. An open channel

develops if the crystallization region is narrow (Spiegelman, 1993c), as occurs within the closely spaced isotherms near the ridge axis.

Assuming primarily vertical melt transport under a buoyancy-dominated regime, Hebert and Montési (2010) predict distinctive crystallization behaviors at different distances off axis for various spreading rates. These differing behaviors result from variations in melt column length and TBL thickness, which influence melt composition. They infer the presence of a permeability barrier at the position of maximum crystallization rate (above a critical threshold value) within each vertical column, corresponding to the appearance of plagioclase \pm clinopyroxene in the crystallizing assemblage. This permeability barrier can be interpreted as a crystallization front, which slopes downward from the spreading center and, depending on the magnitude of the slope, may accommodate melt focusing toward the axis. Melt can travel along the permeability barrier if its slope exceeds a critical value, inferred to be between 0.05 and 0.10 so that the crust is 6 or 7 km thick at most spreading rates. At spreading rates slower than $\sim 40 \text{ mm yr}^{-1}$, characterized by a weaker crystallization front, melt transport to the axis may require an alternative mechanism.

Montési and Behn (2007) proposed that a permeability barrier develops at temperatures of $1,240^\circ\text{C} + 1.9z$, where z is the depth below the surface expressed in kilometers. The thermodynamic modeling of Hebert and Montési (2010) confirmed that relation when the crystallization front is shallower than $\sim 23 \text{ km}$ and associated with the plagioclase multiple saturation point. Underneath the ridge axis, the

permeability barrier is at a depth of $\sim 5 k/V$, where k is the thermal diffusivity of the mantle and V the effective spreading rate (Montési and Behn, 2007). Therefore, the permeability barrier is below the crust at spreading rates less than $\sim 25 \text{ mm yr}^{-1}$. Crustal thickness decreases dramatically and crustal accretion becomes inefficient at ultraslow spreading centers when the effective full-spreading rate is less than 6.5 mm yr^{-1} and the permeability barrier deeper than $\sim 25 \text{ km}$. The transition from slow to ultraslow spreading morphology may be related to the excessive thickness of the lithosphere that melts must traverse from the permeability barrier to the surface, or to the wholesale disappearance of the permeability barrier.

Models that include a parameterized high-porosity channel as described above typically assume that the thermal structure of the mantle is independent of magmatic flow. While there is no doubt that magma responds to the thermal structure established by plate spreading and heat diffusion, it is also clear that magma transports both sensible and latent heat. Hence, magmatic flow can actively change the thermal structure of the mantle (Hewitt and Fowler, 2008). To investigate this interaction, Katz (2008) developed computational models of mid-ocean ridges based on a classical formulation for the dynamics of magma/mantle flow (McKenzie, 1984), coupled with a consistent theory for energy conservation in a two-phase system with melting and freezing (Figure 2A is an example). These models reinforce the idea that melt focusing, as proposed by Sparks and Parmentier (1991), depends critically on viscous resistance to mantle decompression. This resistance controls the ability of magma to destabilize the

flat interface of the permeability barrier due to a self-reinforcing feedback in which magma pools and deposits latent heat, creating a local temperature perturbation that promotes further magma pooling. Constraints from geochemistry

and crustal thickness suggest that focusing is efficient and, hence, that the resistance to decompaction is large. The existence of off-axis volcanism (Sohn and Sims, 2006), however, is a testament to the fact that not all magma is focused

to the ridge axis.

Katz (2010) extended this energetically consistent, two-phase approach to show that active, buoyancy-driven upwellings beneath a mid-ocean ridge (e.g., Rabinowicz et al., 1984) could have observable effects. Figure 2B illustrates the predicted relationship between spreading rate and crustal thickness, overlain on a global compilation of seismically observed crustal thickness (White et al., 2001). Models of passive, plate-driven upwelling yield curves that are monotonically increasing with spreading, but with diminishing slope at moderate to high rates. The contribution of buoyancy forces is to cause crustal thickness to peak at moderate spreading rates and actually decline at large spreading rates. A corresponding trend may be observed in the data, although given the uncertainties in the measurements, there is a legitimate question of its significance.

Connections Between Melt Focusing and Mantle Geochemistry

A critical issue with geodynamic modeling is that there is a trade-off between the values of model parameters relevant to prediction of a particular output (e.g., crustal thickness). In other words, there is no unique set of parameters representing a best fit for a given solution. For example, changes in mantle potential temperature, melt migration pathways, and variations in mantle source composition all affect the predicted model outputs. Compositional petrologic modeling provides an additional constraint that significantly limits the range of model parameters that can reproduce all physical observations (Cordery and

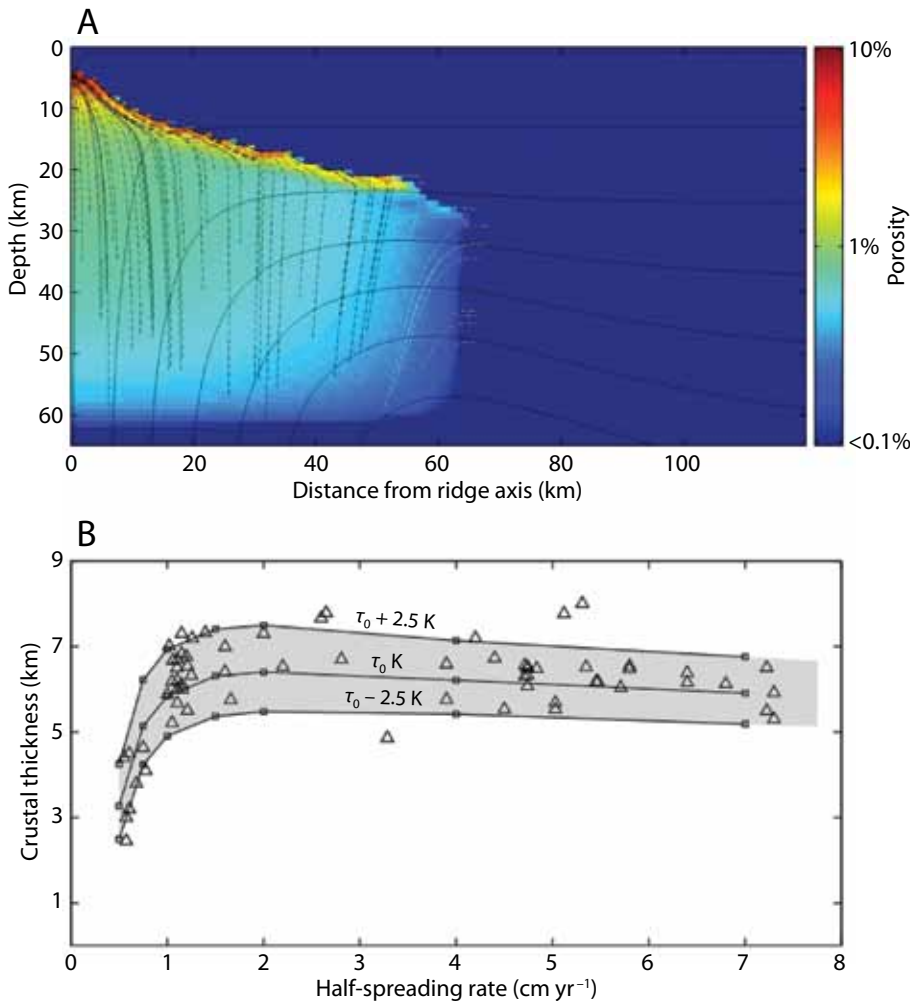


Figure 2. (A) Results of a model simulation after Katz (2010) with half-spreading rate of 4 cm yr^{-1} and a mantle potential temperature of $1,361^\circ\text{C}$ (shown in B). Solid lines are mantle streamlines. Dashed lines are magma streamlines (black are focused to ridge, white are not). (B) Crustal thickness as a function of spreading rate. Data (triangles) are from White et al. (2001). Models (squares + lines) after Katz (2010) compute active mantle flow, melting, and melt migration for a homogeneous mantle. The three curves correspond to three mantle potential temperatures. The large sensitivity of crustal thickness to potential temperature arises because melt focusing pools the difference in melt production over a large area. Crustal thickness has a maximum at $\sim 2\text{ cm yr}^{-1}$ because the relative contribution of buoyancy-driven, active upwelling (compared to plate-driven, passive upwelling) is largest here (see Katz, 2010, for details). The fit to data was achieved by increasing the Clapeyron slope of the solidus, dP/dT , to give a depth of initial melting of $\sim 65\text{ km}$, and reducing the potential temperature ($\tau_0 = 1,633\text{ K}$) to achieve the observed scale of crustal thickness. The height of the melting column sets the length-scale of convection, and is a highly leveraged control on the strength of active upwelling.

Phipps Morgan, 1992, 1993; Shen and Forsyth, 1995; Gregg et al., 2009). For example, higher mantle temperatures cause a deeper onset of melting and higher overall extents of melting, both of which are reflected in basalt composition as well as crustal thickness (Klein and Langmuir, 1987). However, mantle temperature and focusing efficiency trade off to achieve a single crustal thickness value. Specifically, a mantle temperature of 1,350°C with moderately efficient melt focusing may produce the same crustal thickness value as a mantle temperature of 1,325°C and highly efficient melt focusing (Gregg et al., 2009). Melt composition provides additional constraints on geodynamic models. The observed variations in FeO, MgO, and Na₂O, as well as crustal thickness variations, limit the possible range of mantle temperatures and melt focusing distance.

Gregg et al. (2009) combined geodynamic models of the thermal and flow structure of the mantle and the parameterized fractional melting models of Kinzler and Grove (1992a,b, 1993). By calculating melting extent, melt composition, and residual mantle composition at each point in the model space, they directly tested the shape of the melt region and melt migration pathways. For example, the melt region flanks are marked by lower-degree melts originating at greater depth than melts found in the melt region's center directly beneath the ridge axis, with an associated compositional signature. In the first step of this modeling methodology, the temperature structure beneath the spreading ridge is calculated using coupled mantle flow and thermal models (Figure 3A; Shaw et al., 2010). The thermal structure is used to calculate the melt region and melting extent at

each point in the mantle. The latent heat of melting is taken into consideration as it feeds back into the mantle thermal structure. Conductive cooling shuts off melting when the temperature drops below the solidus. The melt is pooled at the top of the melt region where the cumulative melt composition is calculated. Once the melt is pooled, the cool subsolidus temperatures initiate crystallization. Finally, the model-predicted fractional crystallization pathways are plotted for major elements and compared with major element data (Figure 3B–E).

Comparison of model predictions with major element data constrains

model inputs such as mantle temperature and source composition. Figure 3 shows the results of a model run to test our understanding of melting processes at the ultraslow spreading Gakkel Ridge in the Arctic. Assuming a mantle potential temperature of 1,350°C and efficient melt focusing from the entire melting region results in extruded lava compositions that match very well with the major element glass data collected from the ridge (Shaw et al., 2010). Similarly, the predicted pooled melt composition matches well with the melt inclusion data from the same samples (Shaw et al., 2010).

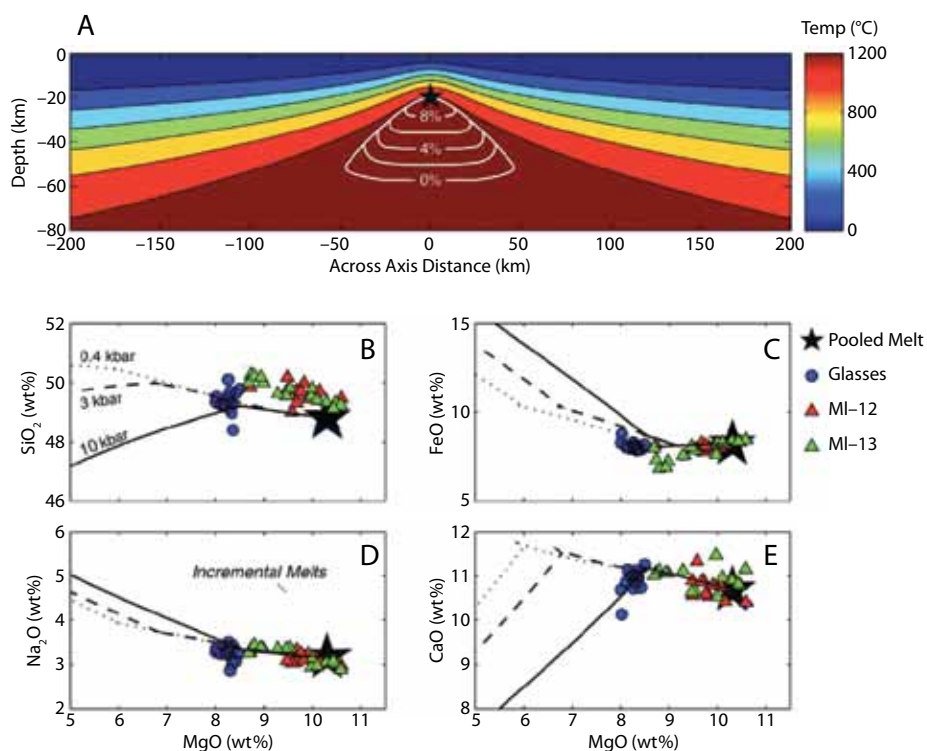


Figure 3. Combining geodynamic models with petrologic models to test the melt region and melt focusing for the ultraslow spreading Gakkel Ridge (Shaw et al., 2010). (A) Passive flow thermal structure for an ultraslow spreading ridge (full spreading rate 10 mm yr⁻¹) with a temperature-dependent visco-plastic rheology. White lines denote melt region calculated from the resultant thermal model using Kinzler and Grove (1992a,b, 1993) with percentages indicating extent of melting. The black star shows the depth of the pooled melt calculation. (B) SiO₂, (C) FeO, (D) Na₂O, and (E) CaO versus MgO for Gakkel glasses (blue circles) and melt inclusions (red and green triangles). Black lines show crystallization paths calculated from Yang et al. (1996) at pressures corresponding to the seafloor (~0.4 kbar; dotted), the maximum saturation pressure recorded in the melt inclusions (3 kbar; dashed), and the mean pressure of melting (10 kbar; solid).

HOW DOES RIDGE SEGMENTATION AFFECT MELT GENERATION AND TRANSPORT?

While the classic conceptualization of the melt-generation region beneath a mid-ocean ridge is a two-dimensional triangle, along-strike variations in ridge structure require a three-dimensional approach. Ridge segmentation is likely to affect the shape and size of the melting region and the migration pathways that melts take to the spreading center. Sophisticated models that combine our knowledge of the geochemical and thermodynamic processes of melt generation with the physics of mantle flow and thermal evolution are needed to address the complexity of melt migration in specific geological examples. Figure 1 illustrates the large region of melt predicted in the mantle beneath the 150 km long Siqueiros Transform Fault that offsets the East Pacific Rise at 8.5°N. The predicted melt region mimics the overlying geometry of the ridge system and jogs beneath the transform fault offset. The cutaway at the northwestern ridge-transform intersection illustrates how the end of the ridge segment not only taps the melt region adjacent to the ridge axis, but also deeper melts generated across the transform fault.

As discussed above, the position of the permeability barrier depends strongly on the predicted thermal structure, which is a function of spreading rate as well as ridge segmentation. A thickened thermal lithosphere beneath transform faults may drive melt toward ridge centers and result in thin crust within the transform fault domain, as observed at slow-spreading centers (Magde et al., 1997). However, observations of local

crustal thickening within the transform domain at intermediate to fast spreading centers (Gregg et al., 2007) and intra-transform spreading centers (ITSCs; Fornari et al., 1989) indicate three-dimensional melt migration and focusing toward the transform fault and extraction within the transform or at ITSCs. Constraining the thermal structure and melt migration pathways in the vicinity of ridge offsets is necessary to better understand the formation of new crust within transform faults.

Hebert and Montési (2011) explored three-dimensional melt migration beneath ridge-transform systems along a parameterized permeability barrier, described above. They infer that melt migration beneath a spreading environment occurs in three stages (Figure 1C): (1) vertical upwelling driven by buoyancy forces within the asthenosphere, (2) buoyancy-driven migration through a high-porosity channel beneath a sloping permeability barrier within the thermal lithosphere, and (3) rapid extraction in shallow melt extraction zones (MEZs) around active plate boundaries where melt extraction is facilitated by structural damage such as faults or dikes intersecting the high-porosity channel. Melt can be extracted to the surface and form new crust if the permeability barrier is shallower than an extraction depth where its slope is less than a critical value, or if melt enters the MEZ, defined in both the vertical and horizontal directions around a plate boundary segment (Montési et al., 2011).

Gregg et al. (2009) and Hebert and Montési (2011) applied the concepts of focusing along a permeability barrier and extraction at an MEZ to the 8–9°N section of the fast-spreading East Pacific Rise (EPR) at the Siqueiros Transform

Fault (Figure 4). Without extraction within an MEZ, a highly heterogeneous crustal structure is predicted along the ridge segments. Regions of anomalously thick crust are predicted 20 to 30 km away from the ridge-transform intersection, consistent with many other models of segmented ridges. These anomalies, which are not observed in actual ridges, may be smoothed out by crustal-level along-axis redistribution (Weatherley and Katz, 2010) or by an MEZ (Hebert and Montési, 2011). An MEZ has the additional effect of allowing melt extraction in the transform domain, producing an anomalously thickened crust consistent with gravity analyses of intermediate to fast spreading ridges (Gregg et al., 2007). In support of this model, the Siqueiros Transform Fault features well-documented recent volcanism, four ITSCs, and several transform-parallel ridges of likely volcanic origin (Fornari et al., 1989). Preferred model parameters include a critical slope less than 0.1, a viscoplastic approximation for brittle weakening, an MEZ extending ~ 10 km from the plate boundary, and an extraction depth of at least 10 km. At slower slipping rates along the transform, the depth of the MEZ required to produce melt redistribution becomes unrealistic, which may explain why crustal thickening is not observed within the transform domains of slow or ultra-slow spreading ridges (Lin et al., 1990; Gregg et al., 2007).

Models incorporating a viscoplastic rheology, which combine a viscous mantle rheology with a brittle rheology for the lithosphere, indicate that the thermal structure of oceanic transform faults offsets may not result in a cold, thick lithosphere (Behn et al., 2007). Behn et al. (2007) find that the

incorporation of a brittle rheology results in elevated temperatures beneath the transform fault offset, which may promote the formation of ITSCs, enhance melting, and encourage the migration of off-axis melt toward the transform fault domain. Furthermore, Gregg et al. (2009) show that using a viscoplastic rheology is necessary to predict the crustal thickness variations observed at segmented transform faults, implying that the presence of ITSCs is not enough to generate the crustal thickness excesses that are observed within intermediate- and fast-slipping transform faults.

Montési et al. (2011) discuss possible melt migration controls and show that a similar three-step scenario can explain variations in crustal thickness at the ultraslow-spreading Southwest Indian Ridge 10–15°E area. There, melt is focused along axis toward two widely spaced seamounts. Montési et al. (2011) show that one of these seamounts corresponds to a region where the permeability barrier has an inverted bowl shape that collects all the melt generated in that region. However, the second seamount requires the presence of an MEZ, as it is located over a region where melt would otherwise migrate eastward. Very little crust, if any, is accreted in the region between the two seamounts, potentially indicating that the permeability barrier is so deep that it does not intersect the MEZ, which is constrained to be 25–30 km deep. This portion of the ridge is cold enough that significant serpentinization is possible, which could mask the gravity signature of the very thin crust. A geophysical investigation of this crucial locality is needed to ascertain whether the lithosphere structure implied by this work is indeed present. This type of study should also

be extended to other segments of the slow-spreading Southwest Indian Ridge, where crustal thickness also records differences in mantle potential temperature (Cannat et al., 2008).

These recent modeling efforts show that at both ultrafast and ultraslow end-members of mid-ocean ridge systems, melt migration can be described as a three-step process of rapid vertical migration, subhorizontal focusing along a permeability barrier, and finally extraction at an MEZ. Undoubtedly, additional processes of ridge migration and composition or temperature-driven

diapirism complicate this simple model (Toomey and Hooft, 2008) and need to be explored in detail in future work.

HOW DOES RIDGE MIGRATION AFFECT MELTING AND MELT FOCUSING?

A feature of classical two-dimensional models of mantle flow beneath ridges is that they are symmetric with respect to the ridge axis. Although this symmetry is a useful conceptual tool, in practice, the mid-ocean ridge system has an abundance of asymmetrical features that cannot be captured by such a model.

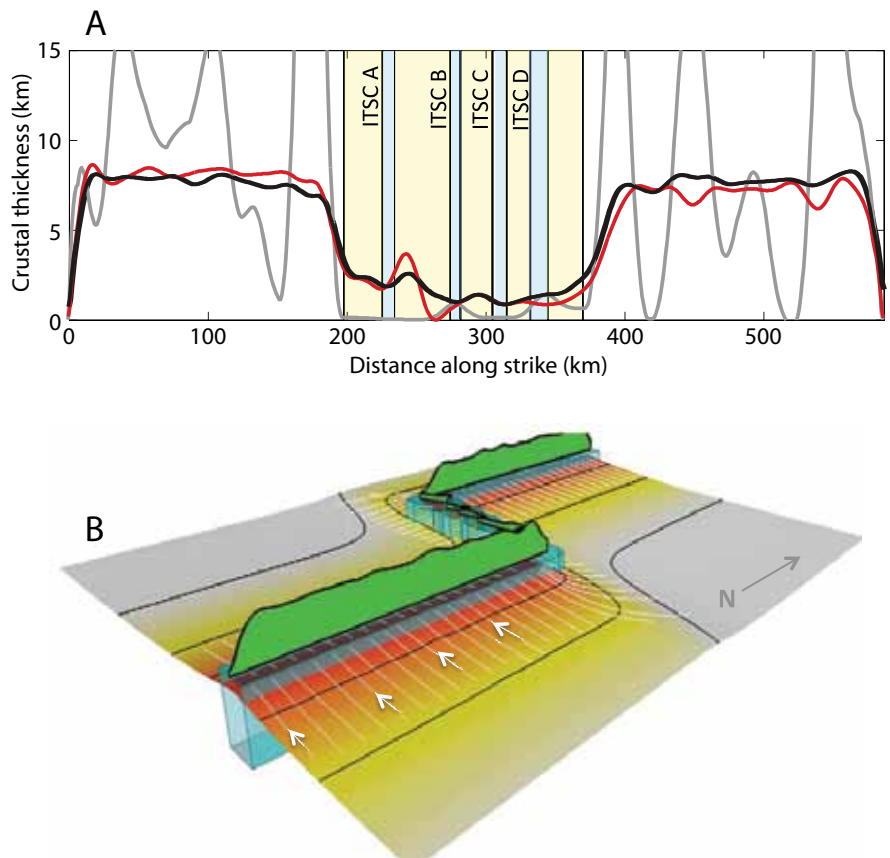


Figure 4. (A) Profile of crustal thickness expected along the East Pacific Rise and the Siqueiros Transform Fault (yellow domains, with intra-transform spreading centers [ITSCs] in blue) for three cases: isoviscous with a 10 km wide melt extraction zone (MEZ; red), isoviscous without an MEZ (gray), and temperature-dependent viscosity with a viscoplastic approximation with a 10 km wide MEZ (black). (B) Three-dimensional rendering of the permeability barrier (color coded, with depth contours every 5 km), the MEZ (translucent blue box), and the profile of instantaneously accreted crustal thickness (green crest). From Hebert and Montési (2011)

We might expect that this asymmetry over the global mid-ocean ridge system would average to zero, allowing it to be considered “noise” on top of the model of flow. However, measurements of axial depth at opposing ends of ridge offsets (e.g., transform faults) provide evidence of systematic asymmetry that is correlated with the direction and magnitude of ridge motion in the hotspot reference frame (Carbotte et al., 2004). In particular, Carbotte et al. (2004) found that of the two ridge segments terminating at an offset in the mid-ocean ridge, the one leading in the direction of ridge migration is consistently shallower, suggesting that there may be a causal relationship between migration and asymmetry.

Several studies have linked asymmetry in mantle upwelling and melting to ridge migration. Davis and Karsten (1986) introduced the idea that the slope of the near-ridge lithosphere-asthenosphere boundary drives a component of asthenospheric flow beneath a migrating ridge: ahead of the migrating ridge, mantle is forced upward, while behind it, mantle is pushed downward. This concept represents a small perturbation to corner flow. The dynamics of this combination were explored in subsequent studies that investigated the effect of ridge migration, pressure gradients, and thermal anomalies on the shape of the melt region (Conder et al., 2002; Toomey et al., 2002; Conder, 2007; Katz, 2010). Carbotte et al. (2004) hypothesized that three-dimensional magmatic focusing, acting on this melting asymmetry, would give rise to the observed pattern of depth asymmetry across ridge offsets. In their scenario, the focusing region associated with the leading segment taps the “upwind” region of enhanced melting, while the focusing region of the trailing

segment taps the “downwind” region of diminished melting. The associated paths of melt migration are inherently three dimensional, and call for models that resolve the three-dimensional thermal and flow structure around ridge offsets. Weatherley and Katz (2010) presented their numerical simulations with these characteristics; their results confirmed earlier predictions and were shown to be consistent with the observations, despite significant scatter in the data. The consistency provides support for the model of magmatic focusing proposed by Sparks and Parmentier (1991).

SUMMARY


Considerable progress has been made in the development and use of geodynamic models to better understand mantle processes at mid-ocean ridges during the Ridge 2000 Program. Advancements such as tracking melt migration through the mantle, calculating melt focusing, and using petrologic modeling have provided a variety of new model constraints. The current diversity of geodynamic modeling approaches and the ability of these models to cross boundaries and integrate both geophysical (Gregg et al., 2007) and geochemical/petrological observations (Shaw et al., 2010) provide the opportunity to examine fundamental questions in mantle dynamics and the formation of new oceanic crust at mid-ocean ridges.

A common feature of recent geodynamical models is the presence of a high-porosity channel at the base of the lithosphere along which melt collects and focuses (Sparks and Parmentier, 1991). The channel may be generated self-consistently (e.g., Katz, 2008) or may follow an approximate parameterization (Hebert and Montési, 2010). Variations

in crustal thickness and lava chemistry are now used to test the importance of segmentation (Gregg et al., 2009; Weatherley and Katz, 2010; Hebert and Montési, 2011; Montési et al., 2011), buoyancy (Katz, 2010), and ridge migration (Toomey et al., 2002; Conder et al., 2002; Katz et al., 2004). New understanding was made possible thanks to the integration of geophysical and geochemical constraints and the detailed modeling of specific key areas to complement global studies.

Many additional features of mid-ocean ridge systems, such as the presence of mantle heterogeneities, including water content and recycled fertile components, variations in mantle temperature, and the possibility of plume influence, suggest important avenues for future work. Key areas for study include slow-spreading ridges such as at the Southwest Indian Ridge, which features clear signals from variations in mantle temperature and hotspot influence, and the East Pacific Rise, where ridge asymmetry is perhaps the most pronounced.

ACKNOWLEDGEMENTS

PMG was supported by a National Science Foundation Graduate Research Fellowship and a Woods Hole Oceanographic Institution Graduate Research Fellowship. LJGM is supported by NSF Grant OCE-0937277. We are grateful for comments by Paul Asimow and Marc Spiegelman. 

REFERENCES

- Aharonov, E., J.A. Whitehead, P.B. Kelemen, and M. Spiegelman. 1995. Channeling instability of upwelling melt in the mantle. *Journal of Geophysical Research* 100:20,433–20,450, <http://dx.doi.org/10.1029/95JB01307>.
- Asimow, P.D., and C.H. Langmuir. 2003. The importance of water to oceanic mantle melting regimes. *Nature* 421:815–820, <http://dx.doi.org/10.1038/nature01429>.

- Behn, M.D., M.S. Boettcher, and G. Hirth. 2007. Thermal structure of oceanic transform faults. *Geology* 35:307–310, <http://dx.doi.org/10.1130/G23112A.1>.
- Buck, W.R., and W. Su. 1989. Focused mantle upwelling below mid-ocean ridges due to feedback between viscosity and melting. *Geophysical Research Letters* 16:641–644, <http://dx.doi.org/10.1029/GL016i007p00641>.
- Bender, J.F., F.N. Hodges, and A.E. Bence. 1978. Petrogenesis of basalts from project FAMOUS area: Experimental study from 0 to 15 kbars. *Earth and Planetary Science Letters* 41:277–302, [http://dx.doi.org/10.1016/0012-821X\(78\)90184-X](http://dx.doi.org/10.1016/0012-821X(78)90184-X).
- Canales, J.P., R. Detrick, D.R. Toomey, and S.D. Wilcock. 2003. Segment-scale variations in the crustal structure of 150–300 kyr old fast spreading oceanic crust (East Pacific Rise, 8°15'N–10°5'N) from wide-angle seismic refraction profiles. *Geophysical Journal International* 152:766–794, <http://dx.doi.org/10.1046/j.1365-246X.2003.01885.x>.
- Cannat, M., D. Sauter, A. Bezos, C. Meyzen, E. Humler, and M. Le Rigoleur. 2008. Spreading rate, spreading obliquity, and melt supply at the ultraslow spreading Southwest Indian Ridge. *Geochemistry Geophysics Geosystems* 9, Q04002, <http://dx.doi.org/10.1029/2007GC001676>.
- Carbotte, S.M., C. Small, and K. Donnelly. 2004. The influence of ridge migration on the magmatic segmentation of mid-ocean ridges. *Nature* 429:743–746, <http://dx.doi.org/10.1038/nature02652>.
- Conder, J.A. 2007. Dynamically driven mantle flow and shear wave splitting asymmetry across the EPR, MELT area. *Geophysical Research Letters* 34, L16301, <http://dx.doi.org/10.1029/2007GL030832>.
- Conder, J.A., D. Forsyth, and E.M. Parmentier. 2002. Asthenospheric flow and asymmetry of the East Pacific Rise, MELT area. *Journal of Geophysical Research* 107(B12):2,344, <http://dx.doi.org/10.1029/2001JB000807>.
- Cordery, M.J., and J. Phipps Morgan. 1992. Melting and mantle flow beneath a mid-ocean spreading center. *Earth and Planetary Science Letters* 111:493–516, [http://dx.doi.org/10.1016/0012-821X\(92\)90199-6](http://dx.doi.org/10.1016/0012-821X(92)90199-6).
- Cordery, M.J., and J. Phipps Morgan. 1993. Convection and melting at mid-ocean ridges. *Journal of Geophysical Research* 98:419,477–419,503, <http://dx.doi.org/10.1029/93JB01831>.
- Davis, E.E., and J.L. Karsten. 1986. On the cause of the asymmetric distribution of seamounts about the Juan De Fuca Ridge: Ridge-crest migration over a heterogeneous asthenosphere. *Earth and Planetary Science Letters* 79:385–396, [http://dx.doi.org/10.1016/0012-821X\(86\)90194-9](http://dx.doi.org/10.1016/0012-821X(86)90194-9).
- Dick, H.J.B., J. Lin, and H. Schouten. 2003. An ultraslow-spreading class of ocean ridge. *Nature* 426:405–412, <http://dx.doi.org/10.1038/nature02128>.
- Fialko, Y.A., and A.M. Rubin. 1998. Thermodynamics of lateral dike propagation: Implications for crustal accretion at slow spreading mid-ocean ridges. *Journal of Geophysical Research* 103:2,501–2,514, <http://dx.doi.org/10.1029/97JB03105>.
- Fornari, D.J., D.G. Gallo, M.H. Edwards, J.A. Madsen, M.R. Perfit, and A.N. Shor. 1989. Structure and topography of the Siqueiros transform fault system: Evidence for the development of intra-transform spreading centers. *Marine Geophysical Researches* 11:263–299, <http://dx.doi.org/10.1007/BF00282579>.
- Forsyth, D.W. 1993. Crustal thickness and the average depth and degree of melting in fractional melting models of passive flow beneath mid-ocean ridges. *Journal of Geophysical Research* 98:16,073–16,079, <http://dx.doi.org/10.1029/93JB01722>.
- Ghiorso, M.S., and R.O. Sack. 1995. Chemical mass transfer in magmatic processes. IV. A revised and internally consistent thermodynamic model for the interpolation and extrapolation of liquid-solid equilibria in magmatic systems at elevated temperatures and pressures. *Contributions to Mineralogy and Petrology* 119:197–212, <http://dx.doi.org/10.1007/BF00307281>.
- Ghods, A., and J. Arkani-Hamed. 2000. Melt migration beneath mid-ocean ridges. *Geophysical Journal International* 140:687–697, <http://dx.doi.org/10.1046/j.1365-246X.2000.00032.x>.
- Gregg, P.M., M.D. Behn, J. Lin, and T.L. Grove. 2009. The effects of mantle rheology and fault segmentation on melt generation and extraction beneath oceanic transform faults. *Journal of Geophysical Research* 114, B11102, <http://dx.doi.org/10.1029/2008JB006100>.
- Gregg, P.M., J. Lin, M.D. Behn, and L.G.J. Montési. 2007. Spreading rate dependence of gravity anomalies along oceanic transform faults. *Nature* 448:183–187, <http://dx.doi.org/10.1038/nature05962>.
- Hebert, L.B., and L.G.J. Montési. 2010. Generation of permeability barriers during melt extraction at mid-ocean ridges. *Geochemistry Geophysics Geosystems* 11, Q12008, <http://dx.doi.org/10.1029/2010GC003270>.
- Hebert, L.B., and L.G.J. Montési. 2011. Melt extraction pathways at segmented oceanic ridges: Application to the East Pacific Rise at the Siqueiros transform. *Geophysical Research Letters* 38, L11306, <http://dx.doi.org/10.1029/2011GL047206>.
- Hewitt, I.J., and A.C. Fowler. 2008. Partial melting in an upwelling mantle column. *Proceedings of the Royal Society A* 464:2,467–2,491, <http://dx.doi.org/10.1098/rspa.2008.0045>.
- Hewitt, I.J., and A.C. Fowler. 2009. Melt channelization in ascending mantle. *Journal of Geophysical Research* 114, B06210, <http://dx.doi.org/10.1029/2008JB006185>.
- Jokat, W., O. Ritzmann, M.C. Schmidt-Aursch, S. Drachev, S. Gauger, and J. Snow. 2003. Geophysical evidence for reduced melt production on the Arctic ultraslow Gakkel mid-ocean ridge. *Nature* 423:962–965, <http://dx.doi.org/10.1038/nature01706>.
- Katz, R.F. 2008. Magma dynamics with the enthalpy method: Benchmark solutions and magmatic focusing at mid-ocean ridges. *Journal of Petrology* 49:2,099–2,121, <http://dx.doi.org/10.1093/petrology/egn058>.
- Katz, R.F. 2010. Porosity-driven convection and asymmetry beneath mid-ocean ridges. *Geochemistry Geophysics Geosystems* 11, Q0AC07, <http://dx.doi.org/10.1029/2010GC003282>.
- Katz, R.F., M. Spiegelman, and S.M. Carbotte. 2004. Ridge migration, asthenospheric flow and the origin of magmatic segmentation in the global mid-ocean ridge system. *Geophysical Research Letters* 31, L15605, <http://dx.doi.org/10.1029/2004GL020388>.
- Katz, R.F., M. Spiegelman, and B. Holtzman. 2006. The dynamics of melt and shear localization in partially molten aggregates. *Nature* 442:676–679, <http://dx.doi.org/10.1038/nature05039>.
- Kelemen, P.B., and E. Aharonov. 1998. Periodic formation of magma fractures and generation of layered gabbros in the lower crust beneath oceanic spreading ridges. Pp. 267–289 in *Faulting and Magmatism at Mid-Ocean Ridges*. W.R. Buck, P.T. Delaney, J.A. Karson, and Y. Lagabrielle, eds, Geophysical Monograph Series, vol. 106, American Geophysical Union, Washington, DC, <http://dx.doi.org/10.1029/GM106p0267>.
- Kelemen, P.B., N. Shimizu, and V.J.M. Salters. 1995. Extraction of mid-ocean ridge basalt from the upwelling mantle by focused flow of melt in dunite channels. *Nature* 375:747–753, <http://dx.doi.org/10.1038/375747a0>.
- Kinzler, R.J., and T.L. Grove. 1992a. Primary magmas of mid-ocean ridge basalts 1. Experiments and methods. *Journal of Geophysical Research* 97:6,885–6,906, <http://dx.doi.org/10.1029/91JB02840>.
- Kinzler, R.J., and T.L. Grove. 1992b. Primary magmas of midocean ridge basalts 2. Applications. *Journal of Geophysical Research* 97:6,907–6,926, <http://dx.doi.org/10.1029/91JB02841>.
- Kinzler, R.J., and T.L. Grove. 1993. Corrections and further discussion of the primary magmas of mid-ocean ridge basalts, 1 and 2. *Journal of Geophysical Research* 98:22,339–22,347, <http://dx.doi.org/10.1029/93JB02164>.
- Kuo, B.Y., and D.W. Forsyth. 1988. Gravity anomalies of the ridge transform intersection system in the South Atlantic between 31 and 34.5°S: Upwelling centers and variations in crustal thickness. *Marine Geophysical Researches* 10:205–232, <http://dx.doi.org/10.1007/BF00310065>.
- Langmuir, C.H., and D.W. Forsyth. 2007. Mantle melting beneath mid-ocean ridges. *Oceanography* 20(1):78–89, <http://dx.doi.org/10.5670/oceanog.2007.82>.

- Langmuir, C.H., J.F. Bender, and R. Batiza. 1986. Petrological and tectonic segmentation of the East Pacific Rise, 5°30'–14°30'N. *Nature* 322:422–429, <http://dx.doi.org/10.1038/322422a0>.
- Lin, J., and J. Phipps Morgan. 1992. The spreading rate dependence of three-dimensional mid-ocean ridge gravity structure. *Geophysical Research Letters* 19:13–16, <http://dx.doi.org/10.1029/91GL03041>.
- Lin, J., G.M. Purdy, H. Schouten, J.-C. Sempere, and C. Zervas. 1990. Evidence from gravity data for focused magmatic accretion along the Mid-Atlantic Ridge. *Nature* 344:627–632, <http://dx.doi.org/10.1038/344627a0>.
- Macdonald, K.C. 1982. Mid-ocean ridges: Fine scale tectonic, volcanic and hydrothermal processes within the plate boundary zone. *Annual Review of Earth and Planetary Sciences* 10:155–190, <http://dx.doi.org/10.1146/annurev.ea.10.050182.001103>.
- Magde, L.S., and D.W. Sparks. 1997. Three-dimensional mantle upwelling, melt generation, and melt migration beneath segment slow spreading ridges. *Journal of Geophysical Research* 102:20,571–20,583.
- Magde, L.S., D.W. Sparks, and R.S. Detrick. 1997. The relationship between buoyant mantle flow, melt migration, and gravity bull's eyes at the Mid-Atlantic Ridge between 33°N and 35°N. *Earth and Planetary Science Letters* 148:59–67, [http://dx.doi.org/10.1016/S0012-821X\(97\)00039-3](http://dx.doi.org/10.1016/S0012-821X(97)00039-3).
- McKenzie, D. 1984. The generation and compaction of partially molten rock. *Journal of Petrology* 25(3):713–765, <http://dx.doi.org/10.1093/petrology/25.3.713>, <http://dx.doi.org/10.1093/petrology/25.3.713>
- MELT Seismic Team. 1998. Imaging the deep seismic structure beneath a mid-ocean ridge: The MELT experiment. *Science* 280:1,215–1,218, <http://dx.doi.org/10.1126/science.280.5367.1215>.
- Montési, L.G.J., and M.D. Behn. 2007. Mantle flow and melting underneath oblique and ultraslow mid-ocean ridges. *Geophysical Research Letters* 34, L24307, <http://dx.doi.org/10.1029/2007GL031067>.
- Montési, L.G.J., M.D. Behn, L.B. Hebert, J. Lin, and J.L. Barry. 2011. Melt focusing at Southwest Indian Ridge 9°–16°E ultraslow spreading center. *Journal of Geophysical Research* 116, B10102, <http://dx.doi.org/10.1029/2011JB008259>.
- Nicolas, A. 1990. Melt extraction from mantle peridotites: Hydrofracturing of porous flow consequences on oceanic ridge activity. Pp. 160–174 in *Magma Transport and Storage*. M.P. Ryan, ed., Wiley, Chichester.
- Phipps Morgan, J. 1987. Melt migration beneath mid-ocean ridge spreading centers. *Geophysical Research Letters* 14:1,238–1,241, <http://dx.doi.org/10.1029/GL014i012p01238>.
- Phipps Morgan, J., and D.W. Forsyth. 1988. Three-dimensional flow and temperature perturbations due to a transform offset: Effects on oceanic crustal and upper mantle structure. *Journal of Geophysical Research* 93:2,955–2,966, <http://dx.doi.org/10.1029/JB093iB04p02955>.
- Rabinowicz, M., A. Nicolas, and J. Vigneresse. 1984. A rolling mill effect in the asthenosphere beneath oceanic spreading centers. *Earth and Planetary Science Letters* 67:97–108, [http://dx.doi.org/10.1016/0012-821X\(84\)90042-6](http://dx.doi.org/10.1016/0012-821X(84)90042-6).
- Reynolds, J.R., and C.H. Langmuir. 1997. Petrological systematics of the Mid-Atlantic Ridge south of Kane: Implications for ocean crust formation. *Journal of Geophysical Research* 102:14,915–14,946, <http://dx.doi.org/10.1029/97JB00391>.
- Reid, I., and H.R. Jackson. 1981. Oceanic spreading rate and crustal thickness. *Marine Geophysical Researches* 5:165–172, <http://dx.doi.org/10.1007/BF00163477>.
- Ribe, N.M., 1988. On the dynamics of mid-ocean ridges. *Journal of Geophysical Research* 93:429–436, <http://dx.doi.org/10.1029/JB093iB01p00429>.
- Scott, D., and D. Stevenson. 1989. A self-consistent model of melting, magma migration, and buoyancy-driven circulation beneath mid-ocean ridges. *Journal of Geophysical Research* 94:2,973–2,988, <http://dx.doi.org/10.1029/JB094iB03p02973>.
- Shaw, A.M., M.D. Behn, S.E. Humphris, R.A. Sohn, and P.M. Gregg. 2010. Deep pooling of low degree melts and volatile fluxes at the 85°E segment of the Gakkel Ridge: Evidence from olivine-hosted melt inclusions and glasses. *Earth and Planetary Science Letters* 288:311–322, <http://dx.doi.org/10.1016/j.epsl.2009.11.018>.
- Shen, Y., and D.W. Forsyth. 1992. The effects of temperature-dependent and pressure-dependent viscosity on three-dimensional passive flow of the mantle beneath a ridge-transform system. *Journal of Geophysical Research* 97:19,717–19,728, <http://dx.doi.org/10.1029/92JB01467>.
- Shen, Y., and D.W. Forsyth. 1995. Geochemical constraints on initial and final depths of melting beneath mid-ocean ridges. *Journal of Geophysical Research* 100:2,211–2,237, <http://dx.doi.org/10.1029/94JB02768>.
- Sleep, N.H. 1988. Tapping of melts by veins and dikes. *Journal of Geophysical Research* 93:10,255–10,272, <http://dx.doi.org/10.1029/JB093iB09p10255>.
- Snow, J.E., and H.N. Edmonds. 2007. Ultraslow-spreading ridges: Rapid paradigm changes. *Oceanography* 20(1):90–101, <http://dx.doi.org/10.5670/oceanog.2007.83>.
- Sohn, R.A., and K.W.W. Sims. 2006. Bending as a mechanism for triggering off-axis volcanism at the East Pacific Rise. *Geology* 33:93–96, <http://dx.doi.org/10.1130/G21116.1>.
- Sparks, D.W., and E.M. Parmentier. 1991. Melt extraction from the mantle beneath spreading centers. *Earth and Planetary Science Letters* 105:368–377, [http://dx.doi.org/10.1016/0012-821X\(91\)90178-K](http://dx.doi.org/10.1016/0012-821X(91)90178-K).
- Sparks, D.W., E.M. Parmentier, and J. Phipps Morgan. 1993. Three-dimensional mantle convection beneath a segmented spreading center: Implications for along-axis variations in crustal thickness and gravity. *Journal of Geophysical Research* 98:21,977–21,995, <http://dx.doi.org/10.1029/93JB02397>.
- Spiegelman, M. 1993a. Flow in deformable porous media: Part 1. Simple analysis. *Journal of Fluid Mechanics* 247:17–38, <http://dx.doi.org/10.1017/S0022112093000369>.
- Spiegelman, M. 1993b. Flow in deformable porous media: Part 2. Numerical analysis—the relationship between shock waves and solitary waves. *Journal of Fluid Mechanics* 247:39–63, <http://dx.doi.org/10.1017/S0022112093000370>.
- Spiegelman, M. 1993c. Physics of melt extraction: Theory, implications and applications. *Philosophical Transactions of the Royal Society of London A* 342:23–41, <http://dx.doi.org/10.1098/rsta.1993.0002>.
- Spiegelman, M., and D. McKenzie. 1987. Simple 2-D models for melt extraction at mid-ocean ridges and island arcs. *Earth and Planetary Science Letters* 83:137–152, [http://dx.doi.org/10.1016/0012-821X\(87\)90057-4](http://dx.doi.org/10.1016/0012-821X(87)90057-4).
- Standish, J.J., and K.W.W. Sims. 2010. Young off-axis volcanism along the ultraslow-spreading Southwest Indian Ridge. *Nature Geoscience* 3:286–292, <http://dx.doi.org/10.1038/ngeo824>.
- Toomey, D.R., and E.E.E. Hooft. 2008. Mantle upwelling, magmatic differentiation, and the meaning of axial depth at fast-spreading ridges. *Geology* 36:679–682, <http://dx.doi.org/10.1130/G24834A.1>.
- Toomey, D.R., W.S.D. Wilcock, J.A. Conder, D.W. Forsyth, J.D. Blundy, E.M. Parmentier, and W.C. Hammond. 2002. Asymmetric mantle dynamics in the MELT region of the East Pacific Rise. *Earth and Planetary Science Letters* 200:287–295, [http://dx.doi.org/10.1016/S0012-821X\(02\)00655-6](http://dx.doi.org/10.1016/S0012-821X(02)00655-6).
- Van Avendonk, H.J.A., A.J. Harding, J.A. Orcutt, and J.S. McClain. 2001. Contrast in crustal structure across the Clipperton Transform Fault from travel time tomography. *Journal of Geophysical Research* 106:10,961–10,981, <http://dx.doi.org/10.1029/2000JB900459>.
- Weatherley, S.M., and R.F. Katz. 2010. Plate-driven mantle dynamics and global patterns of mid-ocean ridge bathymetry. *Geochemistry Geophysics Geosystems* 11, Q10003, <http://dx.doi.org/10.1029/2010GC003192>.
- White, R., T. Minshull, M.J. Bickle, and C. Robinson. 2001. Melt generation at very slow-spreading oceanic ridges: Constraints from geochemical and geophysical data. *Journal of Petrology* 42:1,171–1,196, <http://dx.doi.org/10.1093/petrology/42.6.1171>.
- Yang, H.J., R.J. Kinzler, and T.L. Grove. 1996. Experiments and models of anhydrous, basaltic olivine-plagioclase-augite saturated melts from 0.001 to 10 kbar. *Contributions to Mineralogy and Petrology* 124:1–18, <http://dx.doi.org/10.1007/s004100050169>.
- Zhu, W., G.A. Gaetani, F. Fussteis, L.G.J. Montési, and F. De Carlo. 2011. Microtomography of partially molten rocks: Three-dimensional melt distribution in mantle peridotite. *Science* 332:88–91, <http://dx.doi.org/10.1126/science.1202221>.